References

AGHDAEE, S. R. & RAE, A. I. M. (1983). *J. Chem. Phys.* **49**, 4558.
CARLING, R. W. & WESTRUM, F. F. (1976). *J. Chem. Thermodyn.* **8**, 565–573.
CHOI, C. S. & PRINCE, E. (1976). *J. Chem. Phys.* **64**, 4510–4516.
CROMER, D. T. & MANN, J. B. (1968). *Acta Cryst.* **A24**, 321–324.
IQBAL, Z. (1973). *J. Chem. Phys.* **59**, 1769–1774.
JEFFREY, K. R. (1977). *J. Chem. Phys.* **66**, 4677–4682.
LANGFORD, J. I. & WILSON, A. J. C. (1962). *J. Sci. Instrum.* **39**, 581–585.
PAWLEY, G. S. (1980). *J. Appl. Cryst.* **13**, 630–633.
PRINCE, E. (1981). *J. Appl. Cryst.* **14**, 157–159.
PRINGLE, G. E. & NOAKES, D. E. (1968). *Acta Cryst.* **B24**, 262–269.

RAICH, J. C. & GILLIS, W. S. (1976). *J. Chem. Phys.* **65**, 2088–2094.
RAICH, J. C. & HÜLLER, A. (1979). *J. Chem. Phys.* **70**, 3669–3672.
RIETVELD, H. M. (1969). *J. Appl. Cryst.* **2**, 65–71.
SAKATA, M. & COOPER, M. J. (1979). *J. Appl. Cryst.* **12**, 554–563.
SCOTT, H. G. (1983). *J. Appl. Cryst.* **16**, 159–163.
SHELDRICK, G. M. (1976). *SHELX76*. A program for crystal structure determination. Univ. of Cambridge, England.
SIMONIS, G. J. & HATHAWAY, C. E. (1974). *Phys. Rev. B,* **10**, 4419–4433.
STEVENS, E. D. & HOPE, H. (1977). *Acta Cryst.* **A33**, 723–729.
WADHAWAN, V. K. (1983). *Phase Transitions,* **3**, 3.
WILES, D. B. & YOUNG, R. A. (1981). *J. Appl. Cryst.* **14**, 149–151.
YOUNG, R. A. (1966). *J. Sci. Instrum.* **43**, 449–453.

Synthetic Epsomite, MgSO4.7H2O: Absolute Configuration and Surface Features of the Complementary {111} Forms

BY M. CALLERI, A. GAVETTI, G. IVALDI AND M. RUBBO

Istituto di Mineralogia, Cristallografia e Geochimica dell' Università, Via San Massimo 22, 10123 Torino, Italy

Abstract

Epsomite, $MgSO_4.7H_2O$, $M_r = 246.5$, is orthorhombic, space group $P2_12_12_1$. To establish its absolute configuration, a slab was cut from a laevorotatory crystal, grown under controlled conditions, and used for diffractometer measurements with graphite-monochromatized Cu $K\alpha$ radiation ($\lambda = 1.54178$ Å): $a = 11.876$ (2), $b = 12.002$ (2), $c = 6.859$ (1) Å (parameters obtained and refined from 17 reflexions, $87° \le 2\theta \le 113°$), $V = 977.7$ (2) Å^3, $Z = 4$, $F(000) = 520$, $D_x = 1.67$ Mg m^{-3}, μ(Cu $K\alpha$) = 4.01 mm^{-1}, room temperature. Refinement based on 1602 reflexions, 1292 of which were Friedel pairs. Final R for the correct and incorrect enantiomorphs were 0.0797 and 0.0836 respectively, which, taken with the relative F_o, F_c values of the Friedel pairs and with the results from a test proposed by Rogers [*Acta Cryst.* (1981), A37, 734–741], allow the correct configuration to be assigned at a very high confidence level. To have an accurate, room-temperature, determination, a second refinement was completed with a second crystal and graphite-monochromatized Mo $K\alpha$ radiation ($\lambda = 0.71069$ Å): $a = 11.887$ (2), $b = 12.013$ (2), $c = 6.861$ (1) Å (parameters from 25 reflexions, $23° \le 2\theta \le 55°$), $V = 979.8$ (1) Å^3, $D_x = 1.67$ Mg m^{-3}, μ(Mo $K\alpha$) = 0.42 mm^{-1}. R for the correct and incorrect configurations 0.0300, 0.0307 for 2848 independent reflexions. The absolute configuration has been correlated with crystal morphology and the relative growth rates of the complementary {111} and {$\bar{1}\bar{1}\bar{1}$} forms within the field of low supersaturations. The
surface features account for the predominance of {$\bar{1}\bar{1}\bar{1}$}.

Introduction

One of the problems to be faced when studying the growth from solution of noncentrosymmetric crystals is the determination of the difference ($\Delta P_{hkl} - \Delta P_{\bar{h}\bar{k}\bar{l}}$), where ΔP stands for the variation of P (polarization energy of the crystal surfaces hkl, $\bar{h}\bar{k}\bar{l}$) due to the adsorption of crystal building units coming from the mother phase. ΔP is strictly related to the surface of the crystal faces and, therefore, in the case of noncentrosymmetric crystals, $\Delta P_{hkl} \ne \Delta P_{\bar{h}\bar{k}\bar{l}}$. ΔP does influence the orthogonal-growth rate (R_{hkl}) of a given form. The mean free-path of a building unit on an (hkl) face, x^s_{hkl}, is a function of the total activation energy for the surface diffusion $\Delta G_{s,diff.} = U_s + \Delta P$, U_s being the activation energy for a building unit to diffuse between two adjacent and equivalent surface sites assumed as undeformed, that is as if they belonged to the crystal bulk structure. Monier & Kern's (1956, and references therein) theory leads to the following growth-rate ratio for two complementary forms, within the field of low supersaturation values:

$$\frac{R_{hkl}}{R_{\bar{h}\bar{k}\bar{l}}} = \frac{x^s_{hkl}}{x^s_{\bar{h}\bar{k}\bar{l}}} = \exp\left(-\frac{\Delta P_{hkl} - \Delta P_{\bar{h}\bar{k}\bar{l}}}{2kT}\right). \quad (1)$$

Equation (1) implies that when $\Delta P_{hkl} > \Delta P_{\bar{h}\bar{k}\bar{l}}$, $x^s_{hkl} < x^s_{\bar{h}\bar{k}\bar{l}}$, that is, to a greater polarization of one form corresponds a shorter mean free-path, and therefore

$R_{hkl} < R_{\bar{h}\bar{k}\bar{l}}$. As a consequence $\{hkl\}$ will be more extended than its complementary $\{\bar{h}\bar{k}\bar{l}\}$.* The determination of the term $(\Delta P_{hkl} - \Delta P_{\bar{h}\bar{k}\bar{l}})$ is attainable experimentally either by kinetics measurements on the individual forms or by the observation of the equilibrium crystal habit in pure solutions; provided that the absolute configuration is known, the above difference can also be deduced from theoretical calculations based on the outermost layer relaxation. Given the absolute configuration, the growth morphology of epsomite crystals can be deduced by the Hartman & Perdok (1955) theory and the surface profiles of the complementary forms can be chosen according to their minimum energy (Gavetti, Rubbo & Franchini-Angela, 1983). The present investigation was therefore undertaken to establish the absolute configuration of epsomite, as yet unknown, in order to correlate unambiguously growth morphology and structure. Two refinements of the structure of this mineral are extant: one based on visually estimated X-ray intensities (Baur, 1964) and the other based on neutron diffractometry (Ferraris, Jones & Yerkess, 1973).

Experimental

Crystal habit and optical-rotatory sign

The crystals to be used in the present analysis were grown by recrystallization of synthetic $MgSO_4.7H_2O$ from pure supersaturated aqueous solutions. The habit of the crystal ($\sim 2 \times 2 \times 3$ cm) used for the determination of rotatory sign and of the absolute configuration is shown in Fig. 1: $\{110\}$ is the dominant form, $\{\bar{1}\bar{1}\bar{1}\}$ is much more developed than $\{111\}$, whilst $\{010\}$ has a modest extension as is usual with this hydrated sulphate. The indexing is in accordance with the absolute configuration. For Cu-radiation diffractometry, a fairly large $(0.3 \times 0.3 \times 1.2$ mm) wedge-shaped slab, on which $(1\bar{1}0)$ and $(1\bar{1}1)$ were still recognizable, was cut as sketched in Fig. 1. The sign of the optical-rotatory power was determined under the polarizing microscope on a slice, ~ 2 mm thick, of the above crystal that proved to be laevorotatory. The same crystal was also used to control the relative growth velocities of the two complementary forms within the field of low supersaturations at which it had been maintained since its nucleation. The growth velocities of the $\{\bar{1}\bar{1}\bar{1}\}$ faces, at low supersaturation σ values, were smaller than for the $\{111\}$ faces. The mother solution from which the crystal was obtained and grown was never allowed to take values greater than $\sigma = (C - C_{eq})/C_{eq} = 0.04$ at 298 K, where C and C_{eq} indicate the actual and equilibrium concentra-

tions of the solution with respect to the heptahydrated sulphate. A second crystal ($0.50 \times 0.45 \times 0.65$ mm), to be used for Mo diffractometry, was grown from a solution with $\sigma \simeq 0.08$; its habit was quite similar to that shown in Fig. 1, but $\{010\}$ was missing.

Diffractometric measurements

For the determination of the absolute configuration the slab cut from the crystal of Fig. 1 was sealed in a Lindemann-glass capillary, in order to prevent loss of water, and then mounted on a Nicolet $R3$ diffractometer. The intensity collection (Cu $K\alpha$ radiation) of an adequate number of Friedel pairs was with the ω-scan technique at variable speed: from $1.7°$ min^{-1} for the weakest to $12.0°$ min^{-1} for the strongest reflexions; scan range $1.4°$; left and right backgrounds measured in stationary mode for 0.7 times the peak-scan time. A Cu attenuator was automatically inserted for six reflexions exceeding 60 000 counts s^{-1} on the pre-scan. One standard reflexion: no intensity decrease in the course of the data collection. Two reciprocal-sphere octants hkl and $\bar{h}kl$ explored within $2\theta = 130°$. Total of 1910 reflexions measured; 1620 having $I \geq 2\sigma(I)$ considered as observed (h: 0–13; k: 0–14; l: −8–+8); 18 discarded in the course of the refinement because their intensity was probably affected by casual errors. Empirical absorption correction, based on the ψ-scan method (North, Phillips & Mathews, 1968) and six reflexions, $25° \leq 2\theta \leq 72°$; absorption coefficients 1.00 to 1.85.

To obtain a more accurate refinement, a second crystal was similarly mounted and used for data collection with Mo $K\alpha$ radiation under the above conditions. hkl octant explored within $2\theta = 76°$; 3015 independent reflexions measured; 2874 considered observed (h 0–20; k: 0–20; l: 1−11); 22 out of 24 low-angle reflexions measured with the Cu attenuator and four weak reflexions discarded in the course of the refinement because of poor F_o vs F_c agreement. Absorption correction based on six reflexions, $17° \leq 2\theta \leq 45°$; absorption coefficients 1.00 to 1.28.
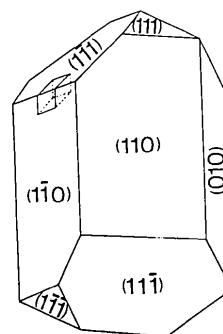
---

* Monier & Kern's (1956) theory was originally developed to interpret growth in the gaseous state, but it seems to hold its validity also for growth from solution (Cadoret, 1965; Abbona, Calleri & Ivaldi, 1984).

Fig. 1. Clinographic projection of the epsomite crystal used for the absolute-configuration determination.

Refinement and determination of the absolute configuration

For all the following computations use was made of the *SHELXTL* system (Sheldrick, 1981). Baur's (1964) parameters were used as a starting model and refined by standard least-squares methods. The scattering factors for neutral atoms were taken from *International Tables for X-ray Crystallography* (1974) and the anomalous-dispersion corrections (Cu $K\alpha$ radiation) for O, Mg and S were introduced from the beginning. The positions of the H atoms were checked on a difference Fourier map at an advanced stage of the anisotropic refinement and found close to Baur's. The introduction of an empirical extinction parameter *nz* (Sheldrick, 1981) was necessary since the strongest reflexions gave evidence of being affected by the secondary-extinction effect. The H-atom coordinates were refined under the initial constraints $W-H = 0.95 \pm 0.01$ Å, $H \cdots H = 1.48 \pm 0.01$ Å; the thermal parameters were set equal to 1.2 times the equivalent U values of the bonded O atoms before each set of cycles (Sheldrick, 1981); at convergence they ranged from 0.03 to 0.05 Å^2. The weighting scheme introduced in the closing cycles was: $1/[\sigma^2(F_o) + GF_o^2]$, where σ is the standard deviation of F_o, based on counting statistics, and G is a variable to be adjusted after each cycle. Under the above conditions two refinements were run: one based on the *xyz* coordinates of Baur's (1964) starting model and the other on the antipodal $1-x$, $1-y$, $1-z$ coordinates (Sheldrick, 1981). At convergence, (mean $\Delta/\sigma \simeq 0.04$) the two refinements yielded respectively: $R = 0.0797$, 0.0836; $wR = 0.0839$, 0.0928; $RG = 0.1016$, 0.1148; $nz = 0.33$ (2), 0.32 (2); $G = 0.0017$, 0.0007, for 1602 reflexions and 161 parameters. The Hamilton test (*International Tables*, 1974, pp. 287–292) favours the first model at the 0.005 confidence level and the scrutiny of the relative trends of F_o and F_c values of the Friedel pairs confirms the choice. Besides, further least-squares cycles were run for both sets of coordinates refining also a parameter which multiplies the imaginary components of the atomic scattering factors [test suggested by Rogers (1981) and included in the *SHELXTL* system]. The chirality is correct if the parameter converges to +1, and *vice versa* if it converges to −1, with a small e.s.d. In our instance this parameter neatly refined to 1.00 (9) and −1.00 (9) for the correct and incorrect chirality respectively; on introducing this parameter the R indices obviously tend to assume the same values. In conclusion, the correct configuration of epsomite may be considered as established at a very high confidence level with reference to the orientation of Figs. 1 and 2. The final R and e.s.d.'s are rather high possibly because of absorption and secondary-extinction effects which are too severe and difficult to correct rigorously, and therefore we carried out a second refinement based

Table 1. *Non-hydrogen-atom coordinates ($\times 10^5$) and equivalent isotropic temperature factors ($\text{Å}^2 \times 10^4$)*

U_{eq} is defined as one third of the trace of the orthogonalized U_{ij} tensor.

	x	y	z	U_{eq}
Mg	42279 (3)	10616 (3)	4023 (6)	181 (1)
S	72658 (2)	18391 (2)	49046 (3)	180 (1)
O(1)	68483 (12)	7519 (8)	42752 (18)	386 (3)
O(2)	85049 (7)	18643 (9)	48316 (15)	305 (2)
O(3)	68864 (8)	20604 (10)	69088 (14)	338 (3)
O(4)	68056 (8)	27242 (8)	36211 (15)	289 (2)
W(1)	26513 (7)	17375 (9)	335 (14)	298 (2)
W(2)	47188 (7)	24819 (7)	19796 (14)	234 (2)
W(3)	46916 (8)	17613 (9)	77947 (14)	295 (2)
W(4)	58271 (8)	4587 (9)	7720 (16)	344 (3)
W(5)	37616 (9)	96138 (7)	88932 (14)	271 (2)
W(6)	36233 (9)	3435 (9)	29140 (15)	323 (2)
W(7)	49164 (10)	43790 (8)	93903 (19)	339 (3)

on a high number of independent reflexions more accurately measured with Mo $K\alpha$ radiation. The H atoms were here allowed more latitude of settlement, the initial constraints being $W-H = 0.95 \pm 0.03$, $H \cdots H = 1.48 \pm 0.04$ Å. After discarding 22 reflexions measured with the attenuator, there was no need to correct for the secondary-extinction effect. The thermal parameters of the H atoms, set equal to 1.2 times the equivalent U's of the bonded O atoms, ranged at convergence (mean $\Delta/\sigma = 0.02$) between 0.03 and 0.04 Å^2. The final agreement parameters for the correct and incorrect chirality were respectively: $R = 0.0300$, 0.0307; $wR = 0.0317$, 0.0328; $RG = 0.0409$, 0.0416; goodness of fit = 1.240, 1.262; $G = 0.00078$, 0.00078 for 2848 reflexions and 160 least-squares parameters; G was kept fixed in the closing cycles. Here the R ratio does not allow safe conclusions (Rogers, 1981). The final difference Fourier map showed only ripples around S, ~ 0.29 e Å^{-3}. Table 1 lists the final parameters for the correct chirality.* Copies of the results from the refinements based on Cu $K\alpha$ radiation are available from the authors.

Discussion

Cleavage

Table 2 gives the relevant interatomic distances and angles, calculated using the cell parameters from Mo $K\alpha$ diffractometry, which are equal to Baur's (1964) only within the rather large standard deviations given by this author. The distances are not corrected for the libration effect; the in-phase correction, however, proved to be small. The positions of the

---

atoms of the asymmetric unit are illustrated in Fig. 2. The results of Tables 1 and 2 are based on the ratio observations/variables = 18, against values of 10 and 3·3 for Baur (1964) and Ferraris et al. (1973) respectively, and therefore the standard deviations are smaller here. Nonetheless the bond distances and angles involving non-hydrogen atoms do not differ significantly and therefore the reader is referred to Baur (1964) and Ferraris et al. (1973) for the description of the structure. Incidentally it may be noted that the differences between the neutron and X-ray parameters are, on the average, smaller for the present refinement than for Baur's. A comment on one of Baur's conclusions is, however, worth giving. Epsomite cleaves perfectly parallel to (010) and distinctly parallel to (101). Baur (1964) explains the cleavage along (010) noting that the four longest hydrogen bonds need to be broken twice per unit cell whilst stronger bonds have to be broken for cleaving along other planes. In point of fact if the cleavage depended only on the number of the broken bonds per unit area, the planes of easiest cleavage would be (010), (110), (201), (101); on considering instead the energy per unit area calculated to break the bonds, the cleavage order would be (110), (201), (010), (101), (021) as shown by Gavetti et al. (1983). Neither sequence corresponds to the observed cleavage order. The discrepancy arises from considering the cleavage dependent on the work of separation only and not on the surface profiles obtainable from the Hartman & Perdok theory. In fact an (hkl) cleavage is related to the shear stress in the (hkl) plane and not to the
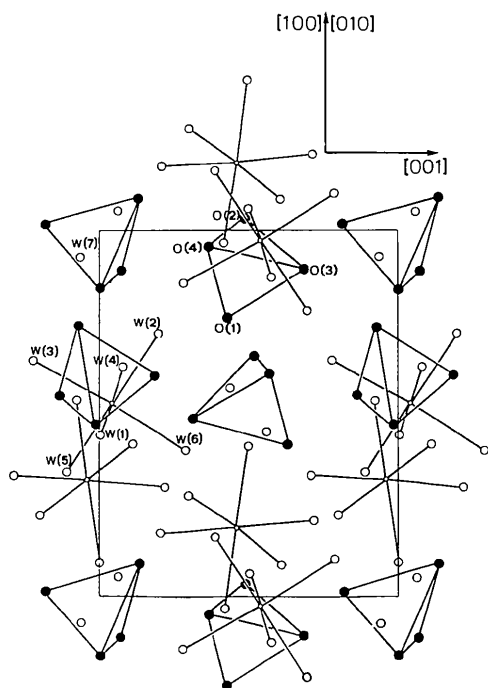

Fig. 2. Projection along [1$\bar{1}$0] of the unit-cell contents.

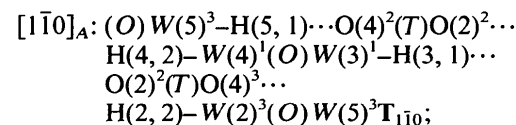Table 2. *Relevant interatomic distances* (Å) *and bond angles* (°), *with e.s.d.'s in parentheses*

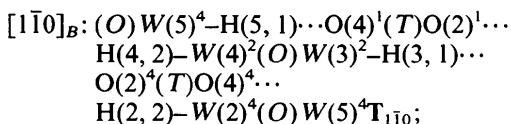| S-O(1)	1·462(1)	O(1)-S-O(2)	110·3(1)
S-O(2)	1·474(1)	O(1)-S-O(3)	109·5(1)
S-O(3)	1·471(1)	O(1)-S-O(4)	109·8(1)
S-O(4)	1·485(1)	O(2)-S-O(3)	109·5(1)
		O(2)-S-O(4)	109·5(1)
		O(3)-S-O(4)	108·2(1)
Mean	1·473(1)	Mean	109·5(1)
O(1)-O(2)	2·410(2)	Mg-W(1)	2·058(1)
O(1)-O(3)	2·395(2)	Mg-W(2)	2·103(1)
O(1)-O(4)	2·412(1)	Mg^i-W(3)	2·052(1)
O(2)-O(3)	2·406(1)	Mg-W(4)	2·050(1)
O(2)-O(4)	2·416(1)	Mg^{ii}-W(5)	2·099(1)
O(3)-O(4)	2·394(1)	Mg-W(6)	2·057(1)
Mean	2·404(1)	Mean	2·070(1)

Superscripts refer to the following positions: (i) $x, y, 1 + z$; (ii) $x, 1 + y, 1 + z$.

orthogonal tensile stress. Therefore, the separation work affords a rough approximation, working well only when the cleavage profile is flat at the atomic scale. It has been shown (Gavetti et al., 1983) that the surface profile of (010) is much smoother than that of (110) whilst the 'saw-tooth' profile of (110) prevents cleavage along this face. All this accounts for the above untenable inversion in the cleavage order.

Surface and growth features of {111} and {$\bar{1}\bar{1}\bar{1}$}

Directions may be singled out in a structure along which uninterrupted periodic sequences (PBC's) of strongly bonded groups develop. Within a slice of thickness d_{hkl} three cases may obtain: (1) no PBC; (2) one PBC; (3) two or more PBC's. The first two instances are not relevant to growth morphology since they correspond to faces of types K and S respectively, i.e. to kinked and stepped profiles. The growth rates of such faces are very high and they tend to disappear from the growth habit. The third case, instead, gives rise to flat faces, F type: their surface profiles remain stable during the growth and their orthogonal-growth rate is the slowest. The analysis of crystal structures and the results from energy calculations show that in some instances more than one PBC, of different stability, can be built up along a given direction, depending on the groups which are selected. Hence combining two independent PBC's to build an F face, one obtains surface profiles and energies that depend on the chosen groups. It is sensible to assume that the more likely surface structure is that resulting from the combination of PBC's which minimize the surface energy. To accomplish this for {111} and {$\bar{1}\bar{1}\bar{1}$} of epsomite (Gavetti et al., 1983), we singled out two chains showing the following sequences:

$[1\bar{1}0]_A$: $(O) W(5)^3$-H(5, 1)$\cdots O(4)^2(T)O(2)^2\cdots$
  H(4, 2)-$W(4)^1(O) W(3)^1$-H(3, 1)$\cdots$
  $O(2)^2(T)O(4)^3\cdots$
  H(2, 2)-$W(2)^3(O) W(5)^3 T_{1\bar{1}0}$;

$[1\bar{1}0]_B$: $(O)W(5)^4$–H$(5, 1)\cdots$O$(4)^1(T)$O$(2)^1\cdots$
　　　　H$(4, 2)$–$W(4)^2(O)W(3)^2$–H$(3, 1)\cdots$
　　　　O$(2)^4(T)$O$(4)^4\cdots$
　　　　H$(2, 2)$–$W(2)^4(O)W(5)^4$T$_{1\bar{1}0}$;

where (O) and (T) indicate octahedral and tetrahedral sites respectively and the superscripts refer to the general equivalent positions of $P2_12_12_1$ in the order given in *International Tables for X-ray Crystallography* (1952): $T_{1\bar{1}0}$ indicates translation along the $[1\bar{1}0]$ axis. Each of these chains is polar and must be paired with its screw-axis equivalent to generate the PBC's of types A and B along $[1\bar{1}0]$, obviously a non-polar direction in epsomite. On considering the slice of thickness $d_{111} = d_{\bar{1}\bar{1}\bar{1}}$, Fig. 3, it is apparent that both the PBC's of type A and of type B are connected by hydrogen bonds along $[10\bar{1}]$ and $[01\bar{1}]$. These latter directions correspond to two other PBC's (Gavetti *et al.*, 1983). Whichever the choice of the PBC, from chain $[1\bar{1}0]_A$ or $[1\bar{1}0]_B$, the faces of forms {111} and {$\bar{1}\bar{1}\bar{1}$} are certainly of type F since in the d_{111} slice two non-equivalent directions of PBC's develop. Starting from a PBC of type A, one obtains surface profiles with two $W(7)$ water molecules on (111) and two on ($\bar{1}\bar{1}\bar{1}$); starting from a PBC of type B, as we did, one obtains all four molecules on ($\bar{1}\bar{1}\bar{1}$) as shown in Fig. 3. This alternative is actually of little consequence as regards the difference between the surface polarization energies of the two complementary forms. In fact {$\bar{1}\bar{1}\bar{1}$}, showing mainly SO_4^{2-} groups
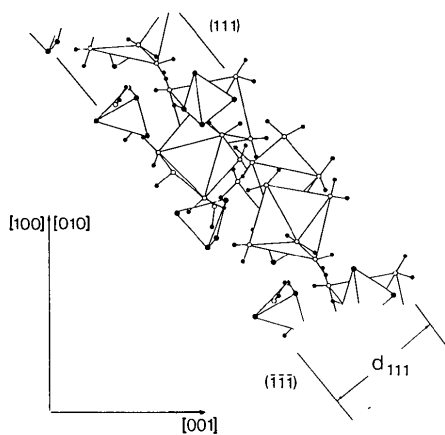
toward the solution, is characterized by a higher polarization energy than {111} where the less polarizable $(Mg.6H_2O)^{2+}$ octahedra outcrop. The latter is the real distinctive feature between the two surfaces. Now, if the $W(7)$ molecules were equally divided between the opposite surfaces, their contribution to $(\Delta P_{\bar{1}\bar{1}\bar{1}} - \Delta P_{111})$ would be virtually null. If all four molecules are on ($\bar{1}\bar{1}\bar{1}$), then the above difference is just slightly increased, as it is clear when considering their effective role during the growth: since $W(7)$ molecules are loosely bonded even inside the crystal, then they must be even less engaged on the crystal surface. Therefore, their probability of being desorbed must be comparable to that of any other water molecule belonging to the commonly adsorbed layer. Taking for granted that $\Delta P_{\bar{1}\bar{1}\bar{1}} > \Delta P_{111}$, from equation (1) it ensues that $R_{\bar{1}\bar{1}\bar{1}} < R_{111}$ as we could experimentally observe for growth at low σ values of supersaturation.

Kinetics investigations on the complementary forms of epsomite, now in progress, based on the determination of the growth isotherms $(R_{111}/R_{\bar{1}\bar{1}\bar{1}})$ for low σ values, will allow the derivation of $(\Delta P_{111} - \Delta P_{\bar{1}\bar{1}\bar{1}})$.

Fig. 3. Projection along $[1\bar{1}0]$ to show the profiles of {111} and {$\bar{1}\bar{1}\bar{1}$}. The $W(7)$ water molecules were all located on the outermost layer of ($\bar{1}\bar{1}\bar{1}$) and they can be seen on the faces of SO_4 tetrahedra.

References

ABBONA, F., CALLERI, M. & IVALDI, G. (1984). *Acta Cryst.* B40, 223–227.
BAUR, H. B. (1964). *Acta Cryst.* 17, 1361–1368.
CADORET, R. (1965). Dr Phys. thesis, Caen Univ.
FERRARIS, G., JONES, D. W. & YERKESS, J. (1973). *J. Chem. Soc.* pp. 816–821.
GAVETTI, A., RUBBO, M. & FRANCHINI-ANGELA, M. (1983). *J. Cryst. Growth*, 57. In the press.
HARTMAN, P. & PERDOK, W. G. (1955). *Acta Cryst.* 8, 49–52, 521–524, 525–529.
International Tables for X-ray Crystallography (1952). Vol. I. Birmingham: Kynoch Press.
International Tables for X-ray Crystallography (1974). Vol. IV. Birmingham: Kynoch Press.
MONIER, J. C. & KERN, R. (1956). *Bull. Soc. Fr. Minéral. Cristallogr.* 79, 495–514.
NORTH, A. C. T., PHILLIPS, D. C. & MATHEWS, F. S. (1968). *Acta Cryst.* A24, 351–359.
ROGERS, D. (1981). *Acta Cryst.* A37, 734–741.
SHELDRICK, G. M. (1981). *SHELXTL. An Integrated System for Solving, Refining and Displaying Crystal Structures from Diffraction Data* (3rd revision). Univ. of Göttingen.